

Exo70 protects against memory and synaptic impairments following mild traumatic brain injury

Matias Lira

UC: Pontificia Universidad Catolica de Chile

Jorge Abarca

UC: Pontificia Universidad Catolica de Chile

Rodrigo G Mira

UC: Pontificia Universidad Catolica de Chile

Pedro Zamorano

University of Antofagasta: Universidad de Antofagasta

Waldo Cerpa (✉ wcerpa@bio.puc.cl)

UC: Pontificia Universidad Catolica de Chile <https://orcid.org/0000-0001-7344-0144>

Research Article

Keywords: traumatic brain injury, Exocyst, Exo70, NMDAR, LTP, memory

Posted Date: October 24th, 2023

DOI: <https://doi.org/10.21203/rs.3.rs-3437728/v1>

License:   This work is licensed under a Creative Commons Attribution 4.0 International License.

[Read Full License](#)

Abstract

Mild traumatic brain injury (mTBI) is damage to the brain due to external forces. It is the most frequent form of brain trauma and a leading cause of disability in young adults. Hippocampal glutamatergic transmission and synaptic plasticity are impaired after mTBI, and NMDA receptors play critical in these functions. The Exocyst is a vesicle tethering complex implicated in the trafficking of glutamate receptors. We have previously shown that Exo70, a critical exocyst's subunit, redistributes in the synapse and increases its interaction with GluN2B in response to mTBI, suggesting a role in the distribution of the GluN2B subunit of NMDARs from synaptic to extrasynaptic membranes. We tested whether Exo70 could prevent NMDAR depletion from the synapse and limit mTBI pathology. To this end, we used a modified Maryland's model of mTBI in mice overexpressing Exo70 in CA1 pyramidal neurons through a lentiviral vector transduction. We showed that after mTBI, the overexpression of Exo70 prevented the cognitive impairment observed in mice infected with a control vector using the Morris' water maze paradigm. Following these findings, mice overexpressing Exo70 showed basal and NMDAR-dependent hippocampal synaptic transmission comparable to sham animals, preventing the deterioration induced by mTBI. Long-term potentiation, abundant synaptic GluN2B-containing NMDARs, and downstream signaling effectors showed that Exo70 overexpression prevented the mTBI-induced alterations. Our findings revealed a crucial role of Exo70 in NMDAR trafficking to the synapse and suggested that the Exocyst complex may be a critical component of the basal machinery that regulates NMDAR distribution in health and disease.

Introduction

Traumatic brain injury (TBI) is an alteration in brain function and physiology caused by external forces leading to brain movement inside the skull [1]. It is a critical health problem worldwide that leads to high medical costs [2] and is recognized as a significant cause of permanent disability and death among young adults [3], with approximately sixty-nine million individuals experiencing TBI worldwide [4]. The most frequent form is mild traumatic brain injury (mTBI), depicting 80–90% of all TBI cases [5–7], resulting in cellular alterations such as axonal disruption, excitotoxicity, oxidative stress, neuroinflammation, neuronal malfunction, cell death, among others [7, 8]. Despite mTBI being the most common, it shares many of these cellular mechanisms with moderate and severe TBI, showing a broad spectrum of cellular responses depending on the severity of the insult and pathophysiology [7].

N-methyl-D-aspartate receptor (NMDAR) is a critical ionotropic glutamate receptor in synaptic plasticity and cognition [9]. It has been extensively studied in several TBI models with proteomics, electrophysiological, and behavioral approaches [7, 8, 10]. Basal synaptic transmission and plasticity decrease upon TBI induction [11, 12], accompanied by a reduction in glutamate binding to receptors [13] and, ultimately, their internalization. In addition, the NMDAR subunit GluN2B availability at synapses is reduced after TBI induction [14, 15], evoking a disbalance in the synaptic/extrasynaptic signaling that triggers detrimental outputs to neurons, which in turn leads to neuronal malfunctioning [16, 17].

The Exocyst is a vesicle tethering protein complex that is comprised of eight subunits: Sec3, Sec5, Sec6, Sec8, Sec10, Sec15, Exo70, and Exo84 [18–20] that oversees the initial contact of secretory vesicles with the plasma membrane during exocytosis [21–24]. Many cellular processes have been associated with the Exocyst, including cell division, membrane growth, cell migration, cell-cell contact, signaling, and tissue morphogenesis, among others [25, 26]. It is required in neuronal development, where it promotes dendritic morphogenesis [27, 28] and axonal elongation [29]. Additionally, it is needed in glutamate receptor trafficking and stabilization in synapses [30, 31].

Exo70 is one of the most studied exocyst subunits and is postulated to be a limiting factor in the functionality of the complex [32, 33]. Exo70 is mainly localized at the plasma membrane [34, 35] and carries the rest of the Exocyst to specific sites where cargo exocytosis is required [36–38]. Exo70 has been shown to participate in neurite development and synapse formation/stabilization [29, 39]. It is also known to interact directly with GluN1 and GluN2B during NMDAR trafficking and delivery into the synapse [31], which is supposedly in charge of basal and stimulated exocytosis [26].

The knowledge of Exocyst's involvement in brain pathologies is minimal. A genetic anomaly of Sec15 and downregulation are involved in neurodevelopmental abnormalities related to language abilities [40–42]. SEC5 and SEC6 variants also affect brain development, presenting severe hypoplastic hippocampi and shrinking cerebellum [43, 44]. Outside those reports, only one has studied Exocyst's involvement in neurodegenerative diseases such as Alzheimer's, where Sec6 has been associated with brain glucose metabolism abnormalities [45].

We previously reported that Exo70 might be associated with mTBI-related synaptic processes due to an Exo70 intracellular redistribution from microsome/plasma membrane fraction into the synaptic compartment [46], where its interaction with GluN2B is increased. In that report, we suggested that the exocyst complex through Exo70 acts as a compensatory mechanism to prevent the exit of NMDARs from the synapse, which impedes the development of mTBI pathology. In the present study, we tested this hypothesis using lentiviral tools to overexpress Exo70 in the hippocampus, which allowed us to assess spatial memory and NMDAR function in mice subjected to mTBI.

Results

We previously showed that Exo70 is redistributed into synapses after a mTBI insult [46]. Exo70 redistribution triggers the exocyst complex assembly in the postsynaptic compartment, where the interaction between Exo70 and GluN2B increases upon mTBI induction. It has been reported that TBI induces the exit of GluN2B from the synapse [14], detrimental to neuron functionality [8]. Thus, we suggested that Exo70 might play a role as a compensatory mechanism stabilizing GluN2B at the postsynaptic density and preventing the development of TBI pathology. To test this hypothesis, we overexpress Exo70 using lentiviral transduction of CA1 neurons (Fig. 1A). The lentivirus used in this work is a third-generation system based on human immunodeficiency, which grants a high biosafety level due to the lack of viral replication capacity. This system allows long-term stable expression of the protein of

interest and does not considerably affect neuronal network activity [49]. Mice injected with lentiviral systems have demonstrated stable lentiviral expression for months, showing even cognitive changes [50–52], and is a reliable tool to use in the research of TBI physiology [53].

2.1 Evaluation of Exo70 overexpression

The bicistronic lentiviral construct expresses a single transcript containing the GFP and the Exo70 ORF. The self-cleavage 1D/2A sequence between GFP and Exo70 ORFs generates both proteins separately with an HA-tagged Exo70 at the N-terminal end (Fig. 1A) [39]. Lentiviral expression was first evaluated in HEK293 cells by immunoblot. The blot analysis showed that GFP is only expressed in the transduced cells, while no GFP signal was detected in non-transduced cells (Fig. 1B). Soluble GFP bands showed two molecular weights, one at 25 kDa corresponding to control LV-GFP lentivirus and the other at ~ 27 kDa. The former is expressed by the control lentivirus (Fig. 1B, arrowhead), and the latter is expressed by HA-tagged Exo70 lentiviral virus (Fig. 1B, asterisk) with the higher molecular weight due to the self-cleavage 1D/2A sequence, which adds residues to the GFP protein and a slight increase in molecular weight is observed [54].

Additionally, a GFP-positive, ~ 96 kDa band was detected only in samples transduced with LV-Exo70, in agreement with what has been reported [39, 54] that approximately 5% of the one-pieced translated protein stays as a single protein without being self-cleaved (Fig. 1B, arrow). After 72h, Exo70 overexpression was achieved only in LV-Exo70 transduced cells (Fig. 1C). Next, the *in vivo* Exo70 overexpression was assessed. Mice were bilaterally injected on postnatal day 30 with 1 µl of lentiviral suspension, and the expression was analyzed 30 days after using dorsal hippocampal samples from injected mice. Similar to HEK293 cells, the analysis showed that GFP is expressed in mice injected with control lentivirus (LV-GFP) and the overexpression lentivirus (LV-Exo70) but was absent in non-injected animals (Fig. 1D); both 25 and 27 kDa bands were observed in these samples as well. The HA tag was only detected in samples from LV-Exo70 mice, indicating that Exo70 is being overexpressed; indeed, 1 month of lentiviral expression was sufficient to increase the Exo70 protein level in the dorsal hippocampus of LV-Exo70, but not LV-GFP injected mice (Fig. 1E). By immunohistochemistry, GFP + cells were found in both LV-GFP and LV-Exo70 injected mice in a wide area of the CA1 region from the dorsal hippocampus (Fig. 1F).

2.2 Learning and Memory

TBI diminished spatial learning and memory [55, 56]. The Morris Water Maze (MWM) assesses spatial memory hippocampal function. For this task, mice must learn the location of a hidden platform based on external cues. Experimental groups' swimming speed was measured to detect possible motor problems. The groups evaluated do not show significant differences (Fig. 2A). Sham-GFP mice showed a typical learning curve as expected for non-injured animals, and mTBI increased escape latency on day 3 and day 4 during the test, while Exo70 overexpression returned escape latency to normal (Fig. 2B). Exo70 overexpression in Sham mice slightly but not significantly improved the escape latency on day 2 and day 4 of the test.

Interestingly, cumulative latency showed that Exo70 overexpression reduced the escape time of both LV-Exo70 Sham/mTBI mice when compared to the control Sham-GFP mice group (Fig. 2C), suggesting that Exo70 overexpression might enhance learning processes in the MWM test. Specifically, on day 4, the results show that Exo70 overexpression rescues the escape latency, as shown in Fig. 2D; representative swimming paths are also shown. Next, we investigated the level of spatial acuity of these animals. Spatial acuity is a more sensitive parameter to measure spatial learning, representing the probability of finding the mice in a specific region around the hidden platform. Figure 2E shows the relationship between spatial acuity and the average escape latency of animals from the different experimental groups. The graph shows that mTBI-GFP mice are located in a region of the graph that corresponds to high-escape latency values and low-spatial acuity scores.

In contrast, Sham-GFP and Sham-Exo70 mice show low-escape latency values and high spatial acuity scores. Exo70 overexpression was able to rescue spatial acuity (Fig. 2E). On day 6 of the memory task, the platform was removed in a probe test that measures the time mice spent swimming in the former area near the initial platform location (a circular area with twice the platform radius). Sham-GFP and Sham-Exo70 mice spent more time in the platform area than TBI-GFP mice, while Exo70 overexpression rescued the memory deficit, demonstrating the inability of mTBI mice to remember the platform location and the improvement in TBI-Exo70 mice (Fig. 2F).

Additionally, animals' cognitive performance was evaluated using a modified spatial memory paradigm associated with episodic memory (memory flexibility), which is more sensitive in detecting hippocampal dysfunction [16]. The analysis of behavioral performance indicates that almost every day, mTBI-GFP mice required more trials to achieve the learning criterion (see Methodology) than control Sham-GFP mice, while Exo70 overexpression prevented learning and memory impairments (Fig. 3A). Figure 3B shows representative swimming paths.

2.3 Synaptic transmission

One of the TBI cellular hallmarks is the alteration of synaptic transmission upon injury induction, both in basal and stimulated transmission. Therefore, we evaluated the total synaptic strength using input/output curves by stimulating Schaffer collaterals with crescent stimuli. A significant decrease in total response to different stimulus intensities was found in mTBI-GFP compared to Sham-GFP mice (Fig. 4A), which were partially rescued by Exo70 intrahippocampal overexpression. Complementary, we evaluated presynaptic function using the paired-pulse facilitation assay, and no differences were found between any of the experimental groups (Fig. 4B).

NMDAR-dependent response in basal synaptic transmission was also assessed by incubating slices in Mg^{2+} -free ACSF with 20 μM NBQX, an AMPAR antagonist, and recording input/output curves. Similar to total response recording, mTBI decreased NMDAR-dependent synaptic response, while overexpression of Exo70 rescued synaptic strength in all stimuli applied (Fig. 4C). Next, synaptic plasticity was evaluated by studying LTP magnitude in hippocampal CA3-CA1 transmission, which also correlates with learning and

memory [57]. Using a high-frequency stimulation protocol (3 trains at 100 Hz). LTP induction was compromised in TBI-GFP compared to Sham-GFP control mice (Fig. 4D). TBI-GFP mice showed potentiation but could not maintain LTP, and Sham-Exo70 mice could induce LTP at a similar proportion as control animals did. Finally, TBI-Exo70 mice could induce and maintain LTP throughout the protocol (Fig. 4D). These results reinforce the rescued memory of the mTBI animals injected with LV-Exo70.

2.4 NMDAR synaptic availability

One of the features of NMDARs is that they can be found both in synaptic and extrasynaptic membranes. Several reports demonstrate that tyrosine phosphorylation of the NMDARs GluN2B subunit is strongly associated with the surface expression of this receptor. For instance, the phosphorylation of tyrosine 1472 determines the surface expression of NMDARs in the synaptic zone [58], and phosphorylated tyrosine 1336 is associated with the enrichment of the receptor in extrasynaptic membranes [59]. Thus, we asked whether the previously observed Exo70-GluN2B increased interaction [46] could be part of a compensatory mechanism by which GluN2B is intended to be stabilized in the synapse since learning/memory and its NMDAR-associated synaptic transmission rescue was allowed by Exo70 overexpression. First, samples from the dorsal hippocampus were analyzed by immunoblot to evaluate the proper expression of the lentiviral construct. Soluble GFP was present in mice from all experimental groups, but only GFP-Exo70 was found in both Sham and mTBI mice injected with LV-Exo70 (Fig. 5A); again, both expected GFP bands (see Fig. 1) were observed in all hippocampal samples. Accordingly, only HA-Exo70 was observed in LV-Exo70 samples, indicating Exo70 overexpression (Fig. 5B).

Using GluN2B p1472 and p1336 antibodies, it was detected that mTBI reduced the p1472 signal compared to control, whereas TBI-Exo70 samples showed a restored signal. Exo70 overexpression in Sham mice did not alter the phosphorylation state of Y1472 (Fig. 5D). Contrary to p1472, mTBI increased the phosphorylation of Y1336, which was partially decreased by Exo70 overexpression. Sham-Exo70 mice showed an apparent increase in the p1336 signal but without statistical significance (Fig. 5E). GluN2B total protein levels did not change in the experimental groups (Fig. 5F). These results suggest that a disbalance of synaptic/extrasynaptic GluN2B occurs with mTBI [15] but also suggest that Exo70 overexpression can retrieve the balance of the synaptic distribution of this NMDAR subunit.

Because an NMDAR synaptic/extrasynaptic disbalance was found, we asked whether these results could correlate with the downstream synaptic signaling through ERK1/2 and CREB. Thus, samples were analyzed using specific antibodies showing phosphorylation of residues related to NMDAR synaptic activity (Fig. 5G). pERK1/2 signal was reduced in mTBI-GFP mice compared to control animals, while mTBI-Exo70 mice showed a restored signal (Fig. 5H). Similar results were observed with the pCREB antibody, where Exo70 overexpression rescued the phosphorylation state of this protein (Fig. 5I). Finally, neither pERK1/2 nor pCREB signal was altered with Exo70 overexpression in Sham animals. These results support the idea that mTBI evokes an exit of GluN2B from the synapse and that the synaptic/extrasynaptic disbalance is restored/prevented when Exo70 is overexpressed.

Discussion

The exocyst complex tethers secretory vesicles during the process of membrane addition for polarized exocytosis [60], and its protein components have been involved in specialized membrane processes in neurons [26]. As such, the Exocyst complex acts as a polymeric unit, providing the molecular machinery to carry on the trafficking and exocytosis of ionotropic glutamate receptors and modulating their availability in the synapse [26, 30, 31]. Here, we report a specific task that the Exocyst performs on an acute neuropathology, like a traumatic brain injury. Previously, we found that Exo70 is redistributed in the hippocampus of mice subjected to mTBI and that the exocyst function might be altered on hippocampal synapses and suggested that NMDARs are stabilized in the synapse by this Exo70 redistribution [46]. To test whether Exo70 redistribution into synapses by increasing its interaction with GluN2B could be a compensatory mechanism to counteract TBI synaptic pathology, we decided to overexpress Exo70 using a lentiviral platform in the CA1 neurons in the dorsal hippocampus, which is related to spatial memory processes [61]. This tool allows a long-term stable expression of the protein of interest and does not considerably affect neuronal network activity [49]. Indeed, around 2 months after the injection, Exo70 overexpression was consistently found in dorsal hippocampal samples (Fig. 1F).

NMDAR synaptic/extrasynaptic balance is of utmost importance in proper synaptic functioning because the intracellular signaling associated with this balance is strictly related to neuronal activity and survival [8]. In animals subjected to mTBI, we found a decrease in the synaptic form of NMDARs (measured by tyrosine 1472 phosphorylation of the GluN2B subunit) and an increase in the population of extrasynaptic NMDARs (measured by tyrosine phosphorylation 1336 of the GluN2B subunit) supporting the idea that mTBI promotes the exit of these receptors from the synapse. This finding agrees with the previous observation using phospho-Y1472 measurement [14] and synaptic compartment localization [15]. Regarding Exo70 overexpression in sham animals, the results showed an enhanced phospho-Y1336 signal, suggesting that a large amount of GluN2B is present in the extrasynaptic compartment; as such, Exo70 should promote GluN2B exocytosis in extrasynaptic membranes. Exo70 mediates AMPAR insertion directly within the postsynaptic density rather than extrasynaptic membranes [30], while NMDARs are inserted into extrasynaptic membranes before being laterally diffused into the synapse. It is then likely that Exo70 has a role in GluN2B insertion at extrasynaptic membranes, as proposed previously [26], both in basal and stimulated NMDAR trafficking. Exo70 prior overexpression in mTBI mice reverted the synaptic/extrasynaptic localization imbalance to what was found in control mTBI mice, suggesting that NMDA synaptic trafficking is reinforced by Exo70 activity, at least in TBI pathophysiology. The observation that Exo70 is redistributed into synapse upon mTBI induction, where it increases its interaction with GluN2B [46], also supports the proposed hypothesis that Exo70 is acting as a compensatory mechanism to relieve/prevent TBI detrimental effects by directly modulating GluN2B synaptic availability.

As previously mentioned, synaptic and extrasynaptic NMDAR have prominent downstream signalings. Synaptic NMDAR low activity decreases phosphorylation levels in CREB, a target of the ERK pathway, reducing neuronal survival (Hardingham et al. 2001; Hardingham and Bading 2002; Hardingham et al. 2002). In TBI, intracellular signaling is complicated to study, and the outcome varies between acute or chronic exposure to trauma-related damage. For example, analysis shortly after the trauma is induced,

typically, an increase in the pCREB signal is observed [62], whereas days to weeks after the insult has occurred, the pCREB signal is strongly dimmed, indicating reduced neuronal survival [63–66]. In our chronic TBI model, we have found a substantial reduction in pCREB and pERK1/2 levels one week after mice were subjected to brain trauma, which agrees with the previous reports already discussed (Fig. 5I). These results show that downstream signaling to the activation of synaptic NMDARs is altered, which also correlates with the GluN2B exit from the synapse, as discussed above. Furthermore, Exo70 overexpression can return the phosphorylation signal in both proteins, supporting the synaptic/extrasynaptic rebalance process of GluN2B.

Synaptic function is essential for the proper performance of the neuronal network. In TBI, hippocampal neuronal circuits are severely affected [67, 68], which impaired basal synaptic transmission [66, 69], as shown in Fig. 4. Exo70 overexpression in the hippocampus prevented hippocampal synaptic transmission loss in mTBI animals, showing that the molecular machinery responsible for the appropriate synaptic functioning is reconstituted in active synapses. On the other hand, Exo70 is a ubiquitous protein present both in pre- and postsynaptic structures [39], suggesting that not only Exo70 carry out a postsynaptic task, but a presynaptic function might be part of the mechanism as well. In this scenario, we did not detect any differences in presynaptic function between all the experimental groups using the paired-pulse facilitation protocol; thus, only the postsynaptic compartment is affected upon mTBI induction in our model, and prevention of damage to synaptic transmission is achieved when Exo70 is overexpressed. Likewise, NMDAR-dependent basal synaptic transmission behaves similarly in mTBI-subjected LV-GFP mice, where transmission is diminished, but only integral prevention is accomplished in NMDAR-dependent transmission as compared to total synaptic transmission, where partial protection is observed. These results suggest that NMDARs are prominent in developing the TBI pathophysiology and that Exo70 is a compensatory mechanism for maintaining synaptic function in the TBI context.

Another aspect of synaptic dysfunction related to TBI is dendritic spine loss/degeneration [70, 71]. These observations have been tightly associated with synaptic transmission impairment [72]. Furthermore, several reports have shown the relationship between spine morphology/function and the exocyst complex. First and foremost, Exo70 is responsible for spine formation and stabilization in cultured hippocampal neurons [39], while the recruitment of the exocyst complex to the postsynaptic compartment by synaptic stimulation triggers the formation of new active synapses [73]. Of note, Exo70 is long thought to be the subunit that leads the Exocyst to the site where it is required. These Exocyst's characteristics suggest that Exo70 overexpression might enhance synapse formation before damage occurs.

Nevertheless, we found no changes in basal synaptic transmission when Exo70 was overexpressed in sham mice. Thus, only an insult such as TBI would activate the exocyst complex to diminish the detrimental effects caused to basal synaptic function. This is supported by the fact that Exo70 is redistributed into the synapse only after mTBI is delivered and promotes the assembly of the Exocyst with GluN2B.

One of the hallmarks of TBI neuropathology is that learning and memory processes are altered upon injury induction. In this regard, NMDARs participate in memory impairment in several TBI models [74–76]. It is important to note that learning and memory strongly correlate with synaptic plasticity in LTP [57], which is also reduced in mild TBI contexts [77, 78]. Our lab has found that NMDAR-related postsynaptic potentials and LTP are reduced upon mTBI induction [15], which concurs with preceding work in the CA1 zone of the hippocampus [78]. Here, we replicated those outcomes and showed that Exo70 overexpression prevented NMDAR-related LTP impairment, suggesting that NMDAR synaptic availability is favored when Exo70 is overexpressed in our mTBI model. However, it is unclear if only GluN2B synaptic stability is responsible for these observations. As synaptic trafficking is enhanced following LTP induction and the Exocyst is a known NMDAR trafficking partner [26], it is plausible to hypothesize that Exo70 enhances NMDAR synaptic trafficking in the mTBI context. Further experiments could address this. Additionally, hippocampal-dependent memory impairment evoked by TBI is associated with the inappropriate activation of the NMDA receptor [74, 79], and its restored activity promotes neuroprotection after TBI [80].

In our hands, the acquisition phase showed that mTBI-GFP mice learned where the platform was more slowly within each test day, whereas Exo70 overexpression prevented the cognitive damage during the acquisition phase. Additionally, Exo70 overexpression in Sham animals slightly enhanced learning in the experimental group, likely due to Exo70's ability to participate in synapse formation, maturation, and maintenance [30, 39]. The same statement applies to Exo70 overexpression in mTBI animals, protecting cognition processes. Moreover, we assessed reference memory with a probe trial 24h after the last acquisition day to ensure memory consolidation in long-term memory was being tested, independent of the memory of the last acquisition session. In this probe trial, Exo70 again protected against cognitive damage and spatial acuity alterations provoked by mTBI. These results suggest that we have found a new Exo70 function in learning and memory processes.

Furthermore, we used the MWM test that conducted reversal phases serially [81], changing the platform to the adjacent quadrant each day of testing, allowing the examination of the animal's flexibility in their ability to learn across multiple phases of new learning [82]. In this regard, memory flexibility is reduced with our mTBI model Fig. 3 and [15], and here, we showed that the impairment is prevented with Exo70 overexpression. It is then likely that in our mTBI model, Exo70 overexpression prevented learning and memory impairments through a cellular process that impedes the exit of NMDAR from the synapse, which keeps synaptic plasticity at a normal level in front of an insult such as TBI.

The summary in Fig. 6 shows that our repeated mTBI protocol induces the exit of GluN2B from synapses, damping its synaptic-related downstream signaling. The diminished NMDAR synaptic localization also reduces total basal glutamatergic transmission and synaptic plasticity and NMDAR-related synaptic transmission and plasticity. The diminished synaptic activity correlates with spatial learning and memory deficits found in mTBI-GFP mice. On the other hand, synaptic NMDARs localization and signaling are retained when Exo70 is overexpressed before mTBI induction. This restored signaling pathway, in turn,

brings back "normal" neuronal activity and survival, granting neurons the ability to act appropriately in the neuronal CA3-CA1 network, as seen by the LTP analysis and the recovery of cognition processes.

Materials and Methods

4.1 Antibodies

Primary antibodies: rabbit Exo70 1:1000 (Proteintech, USA), goat GFP 1:1000 WB; 1:500 IHC (NovusBiologicals, USA), mouse HA 1:1000 (Cell Signalling, USA), mouse Tubulin 1:1000 (NovusBio, USA), mouse β -Actin 1:1000 (Sigma, USA), rabbit GluN2B 1:1000 (Invitrogen, USA), rabbit GluN2B pY1472 1:1000 (Cell Signalling, USA), rabbit GluN2B pY1336 1:1000 (Invitrogen, USA), rabbit pCREB 1:1000 (NovusBiologicals, USA), rabbit pERK1/2 1:1000 (ThermoFisher Scientific, USA), mouse ERK1/2 1:1000 (ThermoFisher Scientific, USA). All secondary antibodies were obtained from Jackson ImmunoResearch, Baltimore, USA.

4.2 Animals

One-month-old C57BL/6J male mice were used in this study. Animals were housed up to 4 mice per cage with a 12:12 hour light/dark cycle (light on at 8:00 am) and provided food and water *ad libitum*. Animals were obtained from CEBIM-UC (Center for Innovation in Biomedical Experimental Models from the Pontificia Universidad Católica de Chile). Animals were handled according to the National Institutes of Health guidelines (NIH Publications No. 8023, revised 1978, Baltimore, MD). All experimental procedures were approved by the Bioethical and Biosafety Committee of the Faculty of Biological Sciences of the Pontificia Universidad Católica de Chile (181009010).

4.3 Lentiviral transduction in HEK293 cells

Third-generation lentiviral particles were packaged and acquired in Applied Biological Materials (ABM, Canada) based on the lentiviral vector FUG-1D2A-Exo70-W [39]. Control lentiviral particles carrying GFP were used as a control. Cells were grown in DMEM supplemented with 10% fetal bovine serum, 100 U/ml ampicillin, and 100 ug/ml streptomycin (Gibco, USA) and maintained at 37°C in an atmosphere of 95% air and 5% CO₂. Cells were transduced with 3 μ l of high titer (1×10^9 IU/ml) lentiviral suspension. Then, 72 h after transduction, cells were harvested for Western blot analysis.

4.4 Intrahippocampal lentiviral injection

One μ l of high titer (1×10^9 IU/ml) lentiviral particles were injected bilaterally into the CA1 *stratum radiatum* region of the dorsal hippocampus from 4 weeks old C57BL/6 J mice using a stereotaxic device. Coordinates from bregma were 1.8 mm caudal, 1.5 mm lateral, and 1.5 mm ventral. The injection rate was 0.5 μ l/min. The syringe was kept inside for 5 min to allow the proper diffusion of lentiviral particles. After surgery, mice were carefully observed in their recovery process in a thermal pad at 37°C. Lentiviral expression was carried out for four weeks.

4.5 Immunohistochemistry

Mice were perfused intracardially with saline solution and PFA 4%. Brains were removed and post-fixed for 6 hours in PFA 4%. 30 μm thick brain slices were cut in a cryostat and stored at -20°C with OLMOS solution. Slices were permeabilized with 0.2% (v/v) Triton X-100 in PBS (PBS-T) for 30 min. Then, a 30 min incubation was carried out with H_2O_2 3% to decrease the background. Slices were washed with PBS-T three times and blocked with 3% BSA for 1 h at room temperature. Slices were incubated overnight at 4°C with GFP primary antibody diluted in PBS-T containing 3% BSA. After three PBS-T washes, slices were incubated with a secondary antibody in PBS-T containing 3% BSA for 2 h at room temperature. Slices were then washed three times with PBS and distilled water. Chromogenic staining was developed using a DAB kit (ThermoFisher Scientific, USA). Finally, slices were mounted on gelatin-coated slides, and images were captured in an Olympus BX51 microscope equipped with a Micro-publisher 3.3 RTV camera (QImaging, Surrey, BC, Canada) using Q-imaging software.

4.6 Western blot analysis

Dorsal hippocampal slices were prepared using a vibratome (BSK microslicer DTK-1500E, Ted Pella, Redding, CA, USA) and immediately processed. Tissues were homogenized in RIPA buffer (10 mM Tris-HCl, Triton X-100 0.5%, 1% NP-40, 5mM EDTA, 1% sodium deoxycholate and 1% SDS) supplemented with protease and phosphatase inhibitor mixture (Protease: Amresco, VWR Life Science; Phosphatase: 25 mM NaF, 100 mM Na_3VO_4 and 30 μM $\text{Na}_4\text{P}_2\text{O}_7$) using a Potter homogenizer and then passing through a tuberculin syringe. Samples were centrifuged at 14,000 rpm at 4°C for 10 min. Protein concentration was determined using a BCA protein assay kit (Pierce, ThermoFisher Scientific, USA). Samples were resolved by SDS-PAGE and transferred to PVDF membranes. Western blot was performed as previously described [46] with overnight incubation of primary antibodies at 4°C . Blots were developed using a chemiluminescence detection kit (Westar Sun, Cyanagen, Italy). Images were obtained with a G:BOX Chemi XT4 Gel imaging system (Syngene).

4.7 Mild traumatic brain injury (mTBI) procedure

To induce mTBI, we used a modified Maryland's weight drop model [47]. For this purpose, we adapted the impact device to fit the mice's anatomy [11, 46]. The impact energy was obtained from a 180-gram steel ball accelerated by gravity along a 1 m rail disposed at a 60° angle from the horizontal. The rail curved at the bottom end to redirect the ball onto a chamber where it struck a coupling arm. The arm then accelerated to impact the malar processes bilaterally with two pistons. After 4 weeks of lentiviral expression, mice were subjected to mTBI. Animals were randomly assigned to receive either sham or mTBI. First, mice were anesthetized with isoflurane using the open-drop method [48]. Animals were then gently restrained onto the impact device using an elastic belt placed across the dorsal thorax, leaving the head free. In a frontal weight impact device, mice were subjected to 5 sessions of 3 blasts each with a 2-day interval. After each session, mice were monitored carefully until the anesthesia effect was finalized

and returned to their home cage. Then, animals were kept in their home cage for 7 days before analysis. Sham animals were subjected to all procedures except injury induction.

4.8 Behavioral tests

The Morris water maze (MWM) task was used as a spatial memory behavioral test. Mice were trained in a 1.1 m diameter circular pool (opaque water, 50 cm deep) filled with 19–21°C water. A submerged 9-cm platform (1 cm below the surface, invisible to the animal) was used for training, with a maximum trial duration of 60 s and 10 s on the platform at the end of the trials. Mice were placed into the water facing the side walls, being transported there by hand from a holding cage. Each animal was trained to locate the platform. The test was performed with three trials per day for 5 days, and a probe test was carried out on day 6 when the platform was removed. Swimming was monitored using an automatic tracking system (ANY-maze video tracking software, Stoelting Co, Wood Dale, IL, USA). This system measured the latency time (in seconds) required for the animal to reach the platform and the time spent in each quadrant (in seconds). After testing, the mouse was gently removed from the maze and returned to its cage.

The week after MWM was performed, memory flexibility was tested using a modified MWM paradigm. Each animal was trained for one pseudo-random platform location daily for 4 days, with a new platform location each day. Up to 15 training trials were performed daily until the criterion of 3 successive trials with an escape latency of < 20 s was met (intertrial delay time = 20 min). Upon testing completion, mice were gently removed from the maze and returned to its cage. The animals were tested for the following location on the following day. Data were collected using a water maze video tracking system (ANY-maze video tracking software, Stoelting Co, Wood Dale, IL, USA).

4.9 Electrophysiology

Transverse slices (400 µm) from the dorsal hippocampus were cut under cold artificial cerebrospinal fluid (ACSF, in mM: 124 NaCl, 2.6 NaHCO₃, 10 D-glucose, 2.69 KCl, 1.25 KH₂PO₄, 2.5 CaCl₂, 1.3 MgSO₄, and 2.60 NaHPO₄) using a Vibratome (BSK microslicer DTK-1500E, Ted Pella, Redding, CA, USA) and incubated in ACSF for 1 hour at room temperature. In all experiments, 10 µM PTX was added to suppress inhibitory GABA_A transmission. Slices were transferred to an experimental chamber (2 ml), superfused (3 ml/min, at room temperature) with gassed ACSF (using 95% O₂/5% CO₂), and visualized by trans-illumination with a binocular microscope (Amscope, Irvine, CA, USA). To evoke field excitatory postsynaptic potentials (fEPSPs), Schaffer collaterals were stimulated with bipolar concentric electrodes (Tungsten, 125 µm OD diameter, Microprobes) connected to an isolation unit (Isoflex, AMPI, Jerusalem, Israel). The stimulation was performed in the *stratum radiatum* within 100–200 µm from the recording site. Recordings were filtered at 2.0–3.0 kHz, sampled at 4.0 kHz using an A/D converter (National Instrument, Austin, TX, USA), and stored with the WinLTP program. The basal excitatory synaptic transmission was measured using an input/output curve protocol with 10 s of the interval between stimuli. We used high-frequency stimulation (HFS) protocol to generate LTP, consisting of 3 trains at 100 Hz stimuli with an inter-train interval of 10 s. In order to isolate NMDAR fEPSP, slices were incubated with

20 μ M NBQX 30 min before testing started, and the antagonist was kept throughout the recording. Data were collected and analyzed offline with pClamp 10 software (Molecular Devices, San Jose, CA, USA).

4.10 Image and Statistical Analysis

Densitometry analysis was carried out with ImageJ (NIH) software, and the data were normalized with specific loading control indicated in each figure legend. All data are expressed as mean \pm SEM. For multiple-grouped experiments, statistical analysis was calculated using one-way ANOVA or two-way ANOVA with Bonferroni correction for multiple comparisons. A $p < 0.05$ value was considered significant. GraphPad Prism 8 was used to carry out statistical analysis.

Declarations

Ethics approval: Animals were handled according to the National Institutes of Health guidelines (NIH Publications No. 8023, revised 1978, Baltimore, MD). All experimental procedures were approved by the Bioethical and Biosafety Committee of the Faculty of Biological Sciences of the Pontificia Universidad Católica de Chile (181009010).

Consent to participate: Not applicable

Consent for publication: Not applicable

Availability of data and materials: The datasets generated during and/or analyzed during the current study are not publicly available due to constants changes in the computational services but are available from the corresponding author on reasonable request”

Competing interests: The authors have no relevant financial or non-financial interests to disclose

Funding: This work has been supported by grants: Agencia Nacional de Investigación y Desarrollo de Chile (ANID), Fondo Nacional de Desarrollo Científico y Tecnológico (FONDECYT) 1190620 to WC, Center for Excellence in Science and Technology (AFB 170005, PFB 12/2007), Sociedad Química y Minera de Chile (SQM) for special grant "The role of lithium on human health and disease" to WC. Ph.D. fellowship was granted by Agencia Nacional de Investigación y Desarrollo (ANID) to ML and RGM. None of the funding sources had any involvement in study design, data collection, preparing the manuscript, or in the decision to submit the manuscript for publication.

Authors' contributions: Conception and design of the study were performed by Matias Lira and Waldo Cerpa. Acquisition and analysis of data were performed by Matias Lira, Jorge Abarca, and Rodrigo G. Mira. Bibliographic research and primary drafting of the manuscript were performed by Matias Lira. Editing and revision of the manuscript were performed by Waldo Cerpa and Pedro Zamorano. All authors approved the final manuscript.

Acknowledgements: We thank researchers from the department of cellular and molecular biology of the faculty of biological sciences of the Pontificia Universidad Católica de Chile, for their willingness to access spaces and equipment under their administration.

References

1. Menon, D. K.; Schwab, K.; Wright, D. W.; Maas, A. I.; Demographics; Clinical Assessment Working Group of the, I.; Interagency Initiative toward Common Data Elements for Research on Traumatic Brain, I.; Psychological, H., Position statement: definition of traumatic brain injury. *Archives of physical medicine and rehabilitation* **2010**, 91, (11), 1637-40.
2. Sabella, S. A.; Andrzejewski, J. H.; Wallgren, A., Financial hardship after traumatic brain injury: a brief scale for family caregivers. *Brain injury* **2018**, 32, (7), 926-932.
3. Roozenbeek, B.; Maas, A. I.; Menon, D. K., Changing patterns in the epidemiology of traumatic brain injury. *Nature reviews. Neurology* **2013**, 9, (4), 231-6.
4. Dewan, M. C.; Rattani, A.; Gupta, S.; Baticulon, R. E.; Hung, Y. C.; Punchak, M.; Agrawal, A.; Adeleye, A. O.; Shrimel, M. G.; Rubiano, A. M.; Rosenfeld, J. V.; Park, K. B., Estimating the global incidence of traumatic brain injury. *Journal of neurosurgery* **2018**, 1-18.
5. Maas, A. I.; Stocchetti, N.; Bullock, R., Moderate and severe traumatic brain injury in adults. *The Lancet. Neurology* **2008**, 7, (8), 728-41.
6. McCrory, P.; Meeuwisse, W.; Aubry, M.; Cantu, B.; Dvorak, J.; Echemendia, R.; Engebretsen, L.; Johnston, K.; Kutcher, J.; Raftery, M.; Sills, A.; Benson, B.; Davis, G.; Ellenbogen, R.; Guskiewicz, K.; Herring, S. A.; Iverson, G.; Jordan, B.; Kissick, J.; McCrea, M.; McIntosh, A.; Maddocks, D.; Makdissi, M.; Purcell, L.; Putukian, M.; Schneider, K.; Tator, C.; Turner, M., Consensus statement on Concussion in Sport - The 4th International Conference on Concussion in Sport held in Zurich, November 2012. *Physical therapy in sport : official journal of the Association of Chartered Physiotherapists in Sports Medicine* **2013**, 14, (2), e1-e13.
7. Blennow, K.; Brody, D. L.; Kochanek, P. M.; Levin, H.; McKee, A.; Ribbers, G. M.; Yaffe, K.; Zetterberg, H., Traumatic brain injuries. *Nature reviews. Disease primers* **2016**, 2, 16084.
8. Carvajal, F. J.; Mattison, H. A.; Cerpa, W., Role of NMDA Receptor-Mediated Glutamatergic Signaling in Chronic and Acute Neuropathologies. *Neural Plast* **2016**, 2016, 2701526.
9. Babaei, P., NMDA and AMPA receptors dysregulation in Alzheimer's disease. *Eur J Pharmacol* **2021**, 908, 174310.
10. Blennow, K.; Hardy, J.; Zetterberg, H., The neuropathology and neurobiology of traumatic brain injury. *Neuron* **2012**, 76, (5), 886-99.
11. Mira, R. G.; Lira, M.; Quintanilla, R. A.; Cerpa, W., Alcohol consumption during adolescence alters the hippocampal response to traumatic brain injury. *Biochem Biophys Res Commun* **2020**, 528, (3), 514-519.

12. Zhang, B.; Chen, X.; Lin, Y.; Tan, T.; Yang, Z.; Dayao, C.; Liu, L.; Jiang, R.; Zhang, J., Impairment of synaptic plasticity in hippocampus is exacerbated by methylprednisolone in a rat model of traumatic brain injury. *Brain research* **2011**, 1382, 165-72.
13. Miller, L. P.; Lyeth, B. G.; Jenkins, L. W.; Oleniak, L.; Panchision, D.; Hamm, R. J.; Phillips, L. L.; Dixon, C. E.; Clifton, G. L.; Hayes, R. L., Excitatory amino acid receptor subtype binding following traumatic brain injury. *Brain research* **1990**, 526, (1), 103-7.
14. Park, Y.; Luo, T.; Zhang, F.; Liu, C.; Bramlett, H. M.; Dietrich, W. D.; Hu, B., Downregulation of Src-kinase and glutamate-receptor phosphorylation after traumatic brain injury. *Journal of cerebral blood flow and metabolism : official journal of the International Society of Cerebral Blood Flow and Metabolism* **2013**, 33, (10), 1642-9.
15. Carvajal, F. J.; Cerpa, W., Regulation of Phosphorylated State of NMDA Receptor by STEP61 Phosphatase after Mild-Traumatic Brain Injury: Role of Oxidative Stress. *Antioxidants (Basel)* **2021**, 10, (10).
16. Carvajal, F. J.; Mira, R. G.; Rovegno, M.; Minniti, A. N.; Cerpa, W., Age-related NMDA signaling alterations in SOD2 deficient mice. *Biochim Biophys Acta Mol Basis Dis* **2018**, 1864, (6 Pt A), 2010-2020.
17. Parsons, M. P.; Raymond, L. A., Extrasynaptic NMDA receptor involvement in central nervous system disorders. *Neuron* **2014**, 82, (2), 279-93.
18. TerBush, D. R.; Maurice, T.; Roth, D.; Novick, P., The Exocyst is a multiprotein complex required for exocytosis in *Saccharomyces cerevisiae*. *The EMBO journal* **1996**, 15, (23), 6483-94.
19. Guo, W.; Grant, A.; Novick, P., Exo84p is an exocyst protein essential for secretion. *The Journal of biological chemistry* **1999**, 274, (33), 23558-64.
20. Hsu, S. C.; Ting, A. E.; Hazuka, C. D.; Davanger, S.; Kenny, J. W.; Kee, Y.; Scheller, R. H., The mammalian brain rsec6/8 complex. *Neuron* **1996**, 17, (6), 1209-19.
21. Pfeffer, S. R., Transport-vesicle targeting: tethers before SNAREs. *Nature cell biology* **1999**, 1, (1), E17-22.
22. Whyte, J. R.; Munro, S., Vesicle tethering complexes in membrane traffic. *Journal of cell science* **2002**, 115, (Pt 13), 2627-37.
23. Guo, W.; Sacher, M.; Barrowman, J.; Ferro-Novick, S.; Novick, P., Protein complexes in transport vesicle targeting. *Trends in cell biology* **2000**, 10, (6), 251-5.
24. Heider, M. R.; Munson, M., Exorcising the exocyst complex. *Traffic* **2012**, 13, (7), 898-907.
25. Martin-Urdiroz, M.; Deeks, M. J.; Horton, C. G.; Dawe, H. R.; Jourdain, I., The Exocyst Complex in Health and Disease. *Frontiers in cell and developmental biology* **2016**, 4, 24.
26. Lira, M.; Mira, R. G.; Carvajal, F. J.; Zamorano, P.; Inestrosa, N. C.; Cerpa, W., Glutamatergic Receptor Trafficking and Delivery: Role of the Exocyst Complex. *Cells* **2020**, 9, (11).
27. Peng, Y.; Lee, J.; Rowland, K.; Wen, Y.; Hua, H.; Carlson, N.; Lavania, S.; Parrish, J. Z.; Kim, M. D., Regulation of dendrite growth and maintenance by exocytosis. *Journal of cell science* **2015**, 128,

(23), 4279-92.

28. Hazuka, C. D.; Foletti, D. L.; Hsu, S. C.; Kee, Y.; Hopf, F. W.; Scheller, R. H., The sec6/8 complex is located at neurite outgrowth and axonal synapse-assembly domains. *The Journal of neuroscience : the official journal of the Society for Neuroscience* **1999**, 19, (4), 1324-34.
29. Dupraz, S.; Grassi, D.; Bernis, M. E.; Sosa, L.; Bisbal, M.; Gastaldi, L.; Jausoro, I.; Caceres, A.; Pfenninger, K. H.; Quiroga, S., The TC10-Exo70 complex is essential for membrane expansion and axonal specification in developing neurons. *J Neurosci* **2009**, 29, (42), 13292-301.
30. Gerges, N. Z.; Backos, D. S.; Rupasinghe, C. N.; Spaller, M. R.; Esteban, J. A., Dual role of the Exocyst in AMPA receptor targeting and insertion into the postsynaptic membrane. *The EMBO journal* **2006**, 25, (8), 1623-34.
31. Sans, N.; Prybylowski, K.; Petralia, R. S.; Chang, K.; Wang, Y. X.; Racca, C.; Vicini, S.; Wenthold, R. J., NMDA receptor trafficking through an interaction between PDZ proteins and the exocyst complex. *Nature cell biology* **2003**, 5, (6), 520-30.
32. Ren, J.; Guo, W., ERK1/2 regulate exocytosis through direct phosphorylation of the exocyst component Exo70. *Developmental cell* **2012**, 22, (5), 967-78.
33. Zhang, C.; Brown, M. Q.; van de Ven, W.; Zhang, Z. M.; Wu, B.; Young, M. C.; Synek, L.; Borchardt, D.; Harrison, R.; Pan, S.; Luo, N.; Huang, Y. M.; Ghang, Y. J.; Ung, N.; Li, R.; Isley, J.; Morikis, D.; Song, J.; Guo, W.; Hooley, R. J.; Chang, C. E.; Yang, Z.; Zarsky, V.; Muday, G. K.; Hicks, G. R.; Raikhel, N. V., Endosidin2 targets conserved exocyst complex subunit EXO70 to inhibit exocytosis. *Proceedings of the National Academy of Sciences of the United States of America* **2016**, 113, (1), E41-50.
34. Liu, J.; Zuo, X.; Yue, P.; Guo, W., Phosphatidylinositol 4,5-bisphosphate mediates the targeting of the Exocyst to the plasma membrane for exocytosis in mammalian cells. *Molecular biology of the cell* **2007**, 18, (11), 4483-92.
35. Moore, B. A.; Robinson, H. H.; Xu, Z., The crystal structure of mouse Exo70 reveals unique features of the mammalian Exocyst. *Journal of molecular biology* **2007**, 371, (2), 410-21.
36. Boyd, C.; Hughes, T.; Pypaert, M.; Novick, P., Vesicles carry most exocyst subunits to exocytic sites marked by the remaining two subunits, Sec3p and Exo70p. *The Journal of cell biology* **2004**, 167, (5), 889-901.
37. Hamburger, Z. A.; Hamburger, A. E.; West, A. P., Jr.; Weis, W. I., Crystal structure of the *S.cerevisiae* exocyst component Exo70p. *Journal of molecular biology* **2006**, 356, (1), 9-21.
38. Ahmed, S. M.; Nishida-Fukuda, H.; Li, Y.; McDonald, W. H.; Gradinaru, C. C.; Macara, I. G., Exocyst dynamics during vesicle tethering and fusion. *Nature communications* **2018**, 9, (1), 5140.
39. Lira, M.; Arancibia, D.; Orrego, P. R.; Montenegro-Venegas, C.; Cruz, Y.; Garcia, J.; Leal-Ortiz, S.; Godoy, J. A.; Gundelfinger, E. D.; Inestrosa, N. C.; Garner, C. C.; Zamorano, P.; Torres, V. I., The Exocyst Component Exo70 Modulates Dendrite Arbor Formation, Synapse Density, and Spine Maturation in Primary Hippocampal Neurons. *Mol Neurobiol* **2019**, 56, (7), 4620-4638.
40. Fruhmesser, A.; Blake, J.; Haberlandt, E.; Baying, B.; Raeder, B.; Runz, H.; Spreiz, A.; Fauth, C.; Benes, V.; Utermann, G.; Zschocke, J.; Kotzot, D., Disruption of EXOC6B in a patient with developmental delay,

- epilepsy, and a de novo balanced t(2;8) translocation. *European journal of human genetics : EJHG* **2013**, 21, (10), 1177-80.
41. Wen, J.; Lopes, F.; Soares, G.; Farrell, S. A.; Nelson, C.; Qiao, Y.; Martell, S.; Badukke, C.; Bessa, C.; Ylstra, B.; Lewis, S.; Isoherranen, N.; Maciel, P.; Rajcan-Separovic, E., Phenotypic and functional consequences of haploinsufficiency of genes from Exocyst and retinoic acid pathway due to a recurrent microdeletion of 2p13.2. *Orphanet journal of rare diseases* **2013**, 8, 100.
42. Borsani, G.; Piovani, G.; Zoppi, N.; Bertini, V.; Bini, R.; Notarangelo, L.; Barlati, S., Cytogenetic and molecular characterization of a de-novo t(2p;7p) translocation involving TNS3 and EXOC6B genes in a boy with a complex syndromic phenotype. *European journal of medical genetics* **2008**, 51, (4), 292-302.
43. Van Bergen, N. J.; Ahmed, S. M.; Collins, F.; Cowley, M.; Vetro, A.; Dale, R. C.; Hock, D. H.; de Caestecker, C.; Menezes, M.; Massey, S.; Ho, G.; Pisano, T.; Glover, S.; Gusman, J.; Stroud, D. A.; Dinger, M.; Guerrini, R.; Macara, I. G.; Christodoulou, J., Mutations in the exocyst component EXOC2 cause severe defects in human brain development. *The Journal of experimental medicine* **2020**, 217, (10).
44. Shalata, A.; Lauhasurayotin, S.; Leibovitz, Z.; Li, H.; Hebert, D.; Dhanraj, S.; Hadid, Y.; Mahroum, M.; Bajar, J.; Egenburg, S.; Arad, A.; Shohat, M.; Haddad, S.; Bakry, H.; Moshiri, H.; Scherer, S. W.; Tzur, S.; Dror, Y., Biallelic mutations in EXOC3L2 cause a novel syndrome that affects the brain, kidney and blood. *Journal of medical genetics* **2019**, 56, (5), 340-346.
45. Miller, J. E.; Shivakumar, M. K.; Lee, Y.; Han, S.; Horgousluoglu, E.; Risacher, S. L.; Saykin, A. J.; Nho, K.; Kim, D.; Alzheimer's Disease Neuroimaging, I., Rare variants in the splicing regulatory elements of EXOC3L4 are associated with brain glucose metabolism in Alzheimer's disease. *BMC medical genomics* **2018**, 11, (Suppl 3), 76.
46. Lira, M.; Zamorano, P.; Cerpa, W., Exo70 intracellular redistribution after repeated mild traumatic brain injury. *Biol Res* **2021**, 54, (1), 5.
47. Kilbourne, M.; Kuehn, R.; Tosun, C.; Caridi, J.; Keledjian, K.; Bochicchio, G.; Scalea, T.; Gerzanich, V.; Simard, J. M., Novel model of frontal impact closed head injury in the rat. *Journal of neurotrauma* **2009**, 26, (12), 2233-43.
48. Risling, T. E.; Caulkett, N. A.; Florence, D., Open-drop anesthesia for small laboratory animals. *The Canadian veterinary journal = La revue veterinaire canadienne* **2012**, 53, (3), 299-302.
49. Minerbi, A.; Kahana, R.; Goldfeld, L.; Kaufman, M.; Marom, S.; Ziv, N. E., Long-term relationships between synaptic tenacity, synaptic remodeling, and network activity. *PLoS biology* **2009**, 7, (6), e1000136.
50. Jeon, S. G.; Kang, M.; Kim, Y. S.; Kim, D. H.; Nam, D. W.; Song, E. J.; Mook-Jung, I.; Moon, M., Intrahippocampal injection of a lentiviral vector expressing neurogranin enhances cognitive function in 5XFAD mice. *Experimental & molecular medicine* **2018**, 50, (3), e461.
51. Kanninen, K.; Heikkinen, R.; Malm, T.; Rolova, T.; Kuhmonen, S.; Leinonen, H.; Yla-Herttuala, S.; Tanila, H.; Levonen, A. L.; Koistinaho, M.; Koistinaho, J., Intrahippocampal injection of a lentiviral vector

- expressing Nrf2 improves spatial learning in a mouse model of Alzheimer's disease. *Proceedings of the National Academy of Sciences of the United States of America* **2009**, 106, (38), 16505-10.
52. Barbash, S.; Hanin, G.; Soreq, H., Stereotactic injection of microRNA-expressing lentiviruses to the mouse hippocampus ca1 region and assessment of the behavioral outcome. *J Vis Exp* **2013**, (76), e50170.
53. Farook, J. M.; Shields, J.; Tawfik, A.; Markand, S.; Sen, T.; Smith, S. B.; Brann, D.; Dhandapani, K. M.; Sen, N., GADD34 induces cell death through inactivation of Akt following traumatic brain injury. *Cell death & disease* **2013**, 4, e754.
54. Torres, V.; Barra, L.; Garces, F.; Ordenes, K.; Leal-Ortiz, S.; Garner, C. C.; Fernandez, F.; Zamorano, P., A bicistronic lentiviral vector based on the 1D/2A sequence of foot-and-mouth disease virus expresses proteins stoichiometrically. *J Biotechnol* **2010**, 146, (3), 138-42.
55. Marschner, L.; Schreurs, A.; Lechat, B.; Mogensen, J.; Roebroek, A.; Ahmed, T.; Balschun, D., Single mild traumatic brain injury results in transiently impaired spatial long-term memory and altered search strategies. *Behavioural brain research* **2019**, 365, 222-230.
56. Xu, X.; Cowan, M.; Beraldo, F.; Schranz, A.; McCunn, P.; Geremia, N.; Brown, Z.; Patel, M.; Nygard, K. L.; Khazaee, R.; Lu, L.; Liu, X.; Strong, M. J.; Dekaban, G. A.; Menon, R.; Bartha, R.; Daley, M.; Mao, H.; Prado, V.; Prado, M. A. M.; Saksida, L.; Bussey, T.; Brown, A., Repetitive mild traumatic brain injury in mice triggers a slowly developing cascade of long-term and persistent behavioral deficits and pathological changes. *Acta neuropathologica communications* **2021**, 9, (1), 60.
57. Whitlock, J. R.; Heynen, A. J.; Shuler, M. G.; Bear, M. F., Learning induces long-term potentiation in the hippocampus. *Science* **2006**, 313, (5790), 1093-7.
58. Xu, F.; Plummer, M. R.; Len, G. W.; Nakazawa, T.; Yamamoto, T.; Black, I. B.; Wu, K., Brain-derived neurotrophic factor rapidly increases NMDA receptor channel activity through Fyn-mediated phosphorylation. *Brain research* **2006**, 1121, (1), 22-34.
59. Goebel-Goody, S. M.; Davies, K. D.; Alvestad Linger, R. M.; Freund, R. K.; Browning, M. D., Phosphoregulation of synaptic and extrasynaptic N-methyl-d-aspartate receptors in adult hippocampal slices. *Neuroscience* **2009**, 158, (4), 1446-59.
60. Wu, B.; Guo, W., The Exocyst at a Glance. *Journal of cell science* **2015**, 128, (16), 2957-64.
61. Lee, S. L. T.; Lew, D.; Wickenheisser, V.; Markus, E. J., Interdependence between dorsal and ventral hippocampus during spatial navigation. *Brain and behavior* **2019**, 9, (10), e01410.
62. Lu, K. T.; Huang, T. C.; Wang, J. Y.; You, Y. S.; Chou, J. L.; Chan, M. W.; Wo, P. Y.; Amstislavskaya, T. G.; Tikhonova, M. A.; Yang, Y. L., NKCC1 mediates traumatic brain injury-induced hippocampal neurogenesis through CREB phosphorylation and HIF-1alpha expression. *Pflugers Archiv : European journal of physiology* **2015**, 467, (8), 1651-61.
63. Rehman, S. U.; Ikram, M.; Ullah, N.; Alam, S. I.; Park, H. Y.; Badshah, H.; Choe, K.; Kim, M. O., Neurological Enhancement Effects of Melatonin against Brain Injury-Induced Oxidative Stress, Neuroinflammation, and Neurodegeneration via AMPK/CREB Signaling. *Cells* **2019**, 8, (7).

64. Zhang, B.; Bai, M.; Xu, X.; Yang, M.; Niu, F.; Gao, F.; Liu, B., Corticosteroid receptor rebalancing alleviates critical illness-related corticosteroid insufficiency after traumatic brain injury by promoting paraventricular nuclear cell survival via Akt/CREB/BDNF signaling. *Journal of neuroinflammation* **2020**, *17*, (1), 318.
65. Atkins, C. M.; Falo, M. C.; Alonso, O. F.; Bramlett, H. M.; Dietrich, W. D., Deficits in ERK and CREB activation in the hippocampus after traumatic brain injury. *Neuroscience letters* **2009**, *459*, (2), 52-6.
66. Titus, D. J.; Wilson, N. M.; Freund, J. E.; Carballosa, M. M.; Sikah, K. E.; Furones, C.; Dietrich, W. D.; Gurney, M. E.; Atkins, C. M., Chronic Cognitive Dysfunction after Traumatic Brain Injury Is Improved with a Phosphodiesterase 4B Inhibitor. *The Journal of neuroscience : the official journal of the Society for Neuroscience* **2016**, *36*, (27), 7095-108.
67. Krishna, G.; Beitchman, J. A.; Bromberg, C. E.; Currier Thomas, T., Approaches to Monitor Circuit Disruption after Traumatic Brain Injury: Frontiers in Preclinical Research. *International journal of molecular sciences* **2020**, *21*, (2).
68. Schumm, S. N.; Gabrieli, D.; Meaney, D. F., Neuronal Degeneration Impairs Rhythms Between Connected Microcircuits. *Frontiers in computational neuroscience* **2020**, *14*, 18.
69. Xu, S. Y.; Liu, M.; Gao, Y.; Cao, Y.; Bao, J. G.; Lin, Y. Y.; Wang, Y.; Luo, Q. Z.; Jiang, J. Y.; Zhong, C. L., Acute histopathological responses and long-term behavioral outcomes in mice with graded controlled cortical impact injury. *Neural regeneration research* **2019**, *14*, (6), 997-1003.
70. Xiong, Y.; Mahmood, A.; Chopp, M., Remodeling dendritic spines for treatment of traumatic brain injury. *Neural regeneration research* **2019**, *14*, (9), 1477-1480.
71. Maiti, P.; Manna, J.; Ilavazhagan, G.; Rossignol, J.; Dunbar, G. L., Molecular regulation of dendritic spine dynamics and their potential impact on synaptic plasticity and neurological diseases. *Neuroscience and biobehavioral reviews* **2015**, *59*, 208-37.
72. Jamjoom, A. A. B.; Rhodes, J.; Andrews, P. J. D.; Grant, S. G. N., The synapse in traumatic brain injury. *Brain* **2021**, *144*, (1), 18-31.
73. Teodoro, R. O.; Pekkurnaz, G.; Nasser, A.; Higashi-Kovtun, M. E.; Balakireva, M.; McLachlan, I. G.; Camonis, J.; Schwarz, T. L., Ral mediates activity-dependent growth of postsynaptic membranes via recruitment of the Exocyst. *The EMBO journal* **2013**, *32*, (14), 2039-55.
74. Han, R. Z.; Hu, J. J.; Weng, Y. C.; Li, D. F.; Huang, Y., NMDA receptor antagonist MK-801 reduces neuronal damage and preserves learning and memory in a rat model of traumatic brain injury. *Neurosci Bull* **2009**, *25*, (6), 367-75.
75. Gabrieli, D.; Schumm, S. N.; Vigilante, N. F.; Meaney, D. F., NMDA Receptor Alterations After Mild Traumatic Brain Injury Induce Deficits in Memory Acquisition and Recall. *Neural computation* **2021**, *33*, (1), 67-95.
76. Biegon, A.; Fry, P. A.; Paden, C. M.; Alexandrovich, A.; Tsenter, J.; Shohami, E., Dynamic changes in N-methyl-D-aspartate receptors after closed head injury in mice: Implications for treatment of neurological and cognitive deficits. *Proceedings of the National Academy of Sciences of the United States of America* **2004**, *101*, (14), 5117-22.

77. Aungst, S. L.; Kabadi, S. V.; Thompson, S. M.; Stoica, B. A.; Faden, A. I., Repeated mild traumatic brain injury causes chronic neuroinflammation, changes in hippocampal synaptic plasticity, and associated cognitive deficits. *Journal of cerebral blood flow and metabolism : official journal of the International Society of Cerebral Blood Flow and Metabolism* **2014**, 34, (7), 1223-32.
78. Schwarzbach, E.; Bonislowski, D. P.; Xiong, G.; Cohen, A. S., Mechanisms underlying the inability to induce area CA1 LTP in the mouse after traumatic brain injury. *Hippocampus* **2006**, 16, (6), 541-50.
79. Cigel, A.; Sayin, O.; Gurgun, S. G.; Sonmez, A., Long term neuroprotective effects of acute single dose MK-801 treatment against traumatic brain injury in immature rats. *Neuropeptides* **2021**, 88, 102161.
80. Sonmez, A.; Sayin, O.; Gurgun, S. G.; Calisir, M., Neuroprotective effects of MK-801 against traumatic brain injury in immature rats. *Neurosci Lett* **2015**, 597, 137-42.
81. Vorhees, C. V.; Williams, M. T., Morris water maze: procedures for assessing spatial and related forms of learning and memory. *Nat Protoc* **2006**, 1, (2), 848-58.
82. Williams, M. T.; Morford, L. L.; Wood, S. L.; Wallace, T. L.; Fukumura, M.; Broening, H. W.; Vorhees, C. V., Developmental D-methamphetamine treatment selectively induces spatial navigation impairments in reference memory in the Morris water maze while sparing working memory. *Synapse* **2003**, 48, (3), 138-48.

Figures

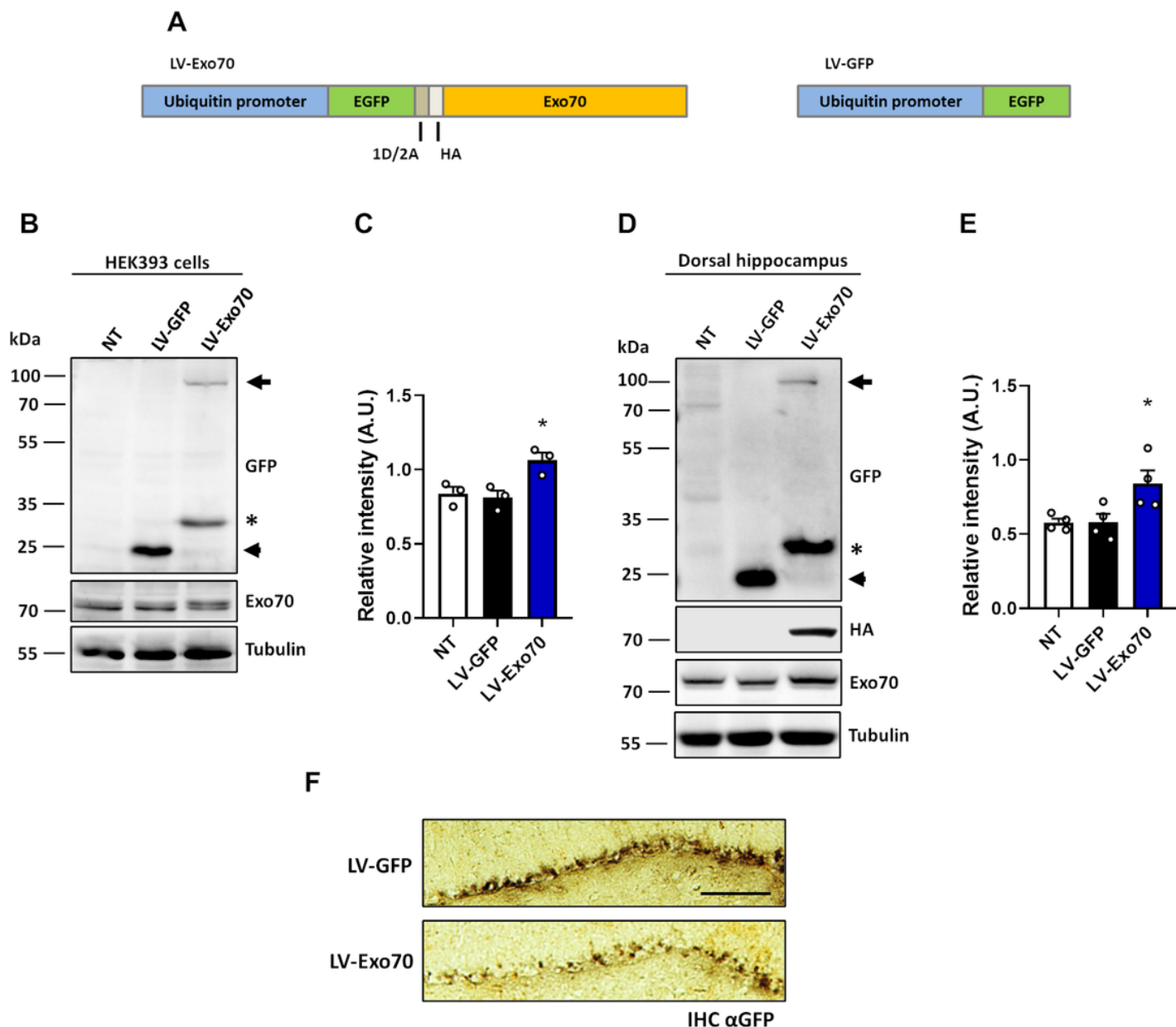


Figure 1

Characterization of the lentiviral system expressing Exo70. (A) Scheme depicting both lentiviral constructs used in this study. (B) Immunoblot analysis of HEK293 cells transduced with 3 μ L of lentiviral suspension. Expression was carried out for 72h. 30 μ g of protein samples were resolved in 10% SDS-PAGE and transferred to PVDF membranes. Membranes were stripped and tested again with the indicated antibodies. (C) One-month-old mice were injected intrahippocampally with 1 μ L of LV-GFP, LV-Exo70 lentiviral suspension, or PBS (NT: non-transduced). Expression was carried out for 30 days. Immunoblot analysis of dorsal hippocampal samples from injected mice. 30 μ g of protein samples were resolved in 10% SDS-PAGE and transferred to PVDF membranes. Membranes were stripped and tested again with the indicated antibodies. (C and E) Densitometric analysis of Exo70. Signal intensity was normalized with Tubulin band intensity. The analyses show Exo70 overexpression only in LV-Exo70 transduced samples.

Values represent means \pm SEM. $n = 3$ independent experiments with HEK293 cells, $n = 4$ mice per experimental group. Statistical differences were determined by an unpaired t-test comparing LV-GFP and LV-Exo70 samples. $*p < 0.05$. **(F)** Classical IHC was carried out using a GFP antibody. Representative images of CA1 hippocampal region showing GFP signal. Scale bar: 100 μ m.

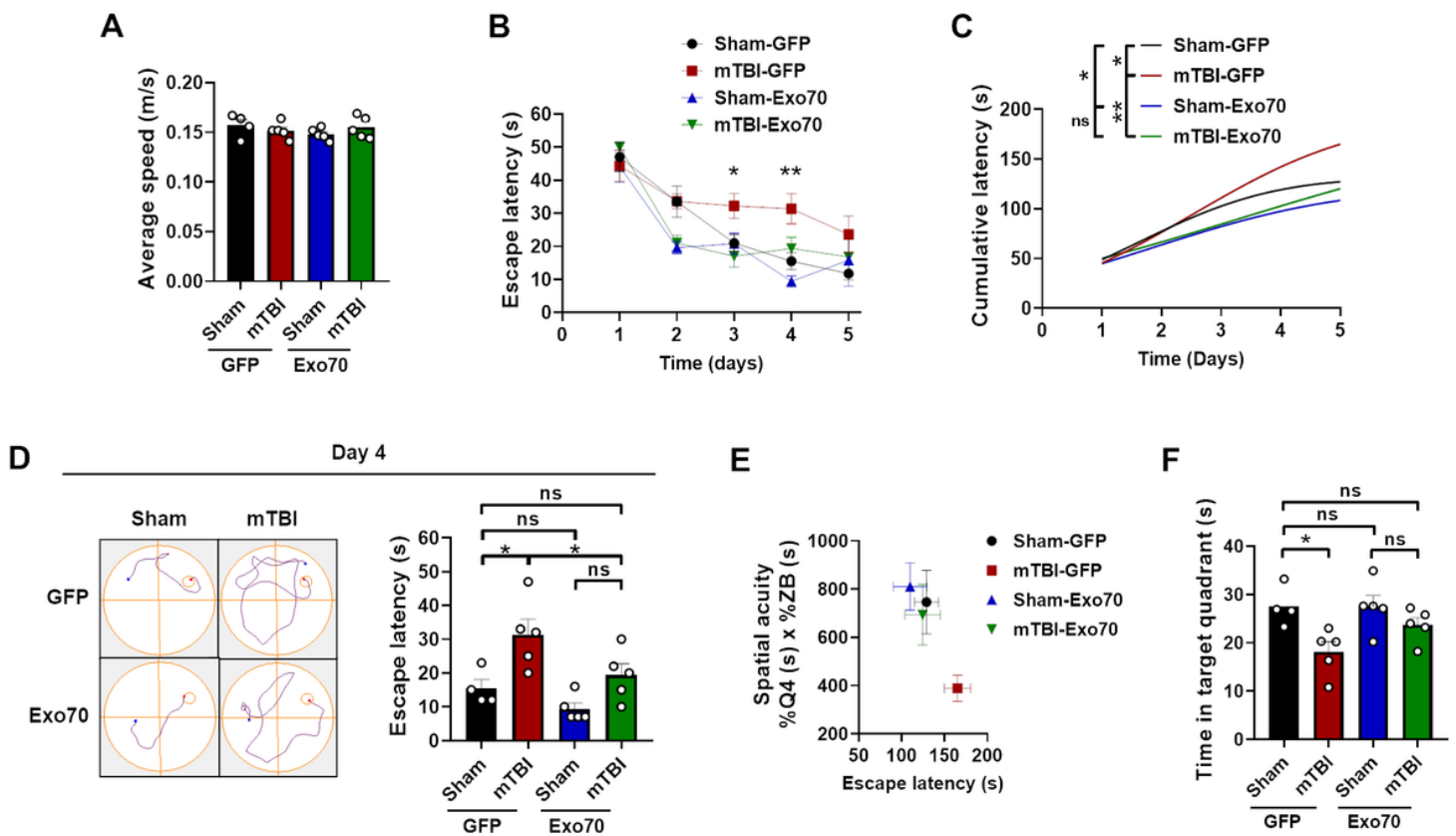


Figure 2

Spatial learning and memory impairment are prevented by Exo70 overexpression in mTBI-induced mice. Behavioral performance was tested using the MWM test. **(A)** Average swimming speed. **(B)** Escape latency (time to reach the hidden platform) of Sham and mTBI mice expressing GFP or Exo70. **(C)** Cumulative latency throughout the 6 days of the test. **(D)** Representative swimming trajectories and escape latency for all experimental groups on day 4. **(E)** Spatial acuity for sham and mTBI mice with or without Exo70 overexpression after 6 training days. **(F)** Analysis of the time mice spent swimming in the area near the platform when it was removed on day 6. Values represent means \pm SEM, $n = 5$ mice per experimental group. Statistical differences were calculated by ANOVA, followed by post hoc Bonferroni's test. Curves were analyzed by Repeated Measures ANOVA. $*p < 0.05$, $**p < 0.01$.

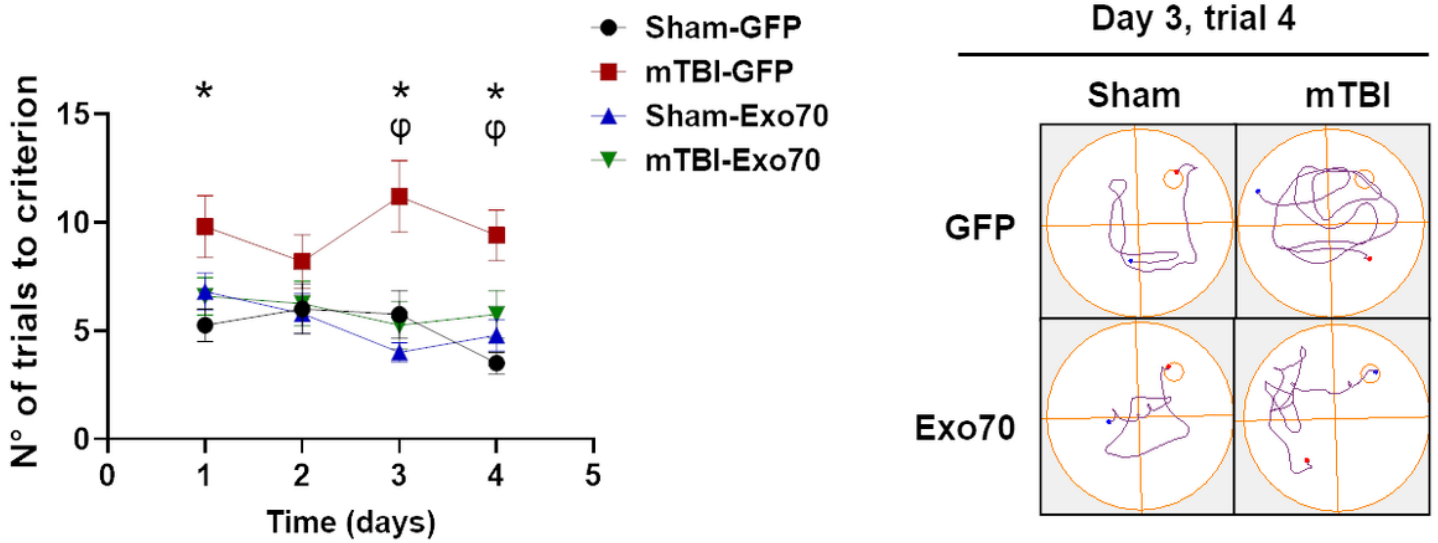


Figure 3

Exo70 overexpression prevents memory flexibility impairment. (A) Behavioral performance was tested using a modification of the MWM, memory flexibility tests (see methods). Memory flexibility was performed the week after the MWM test was carried out. (B) Representative swimming trajectories for trial 4 on day 3 of the test are shown. Values represent means \pm SEM, $n = 5$ mice per experimental group. Statistical differences were calculated by repeated measures ANOVA and post hoc Bonferroni's test. Sham-GFP/TBI-GFP comparison: $*p < 0.05$. TBI-GFP/TBI-Exo70 comparison: $\phi p < 0.05$.

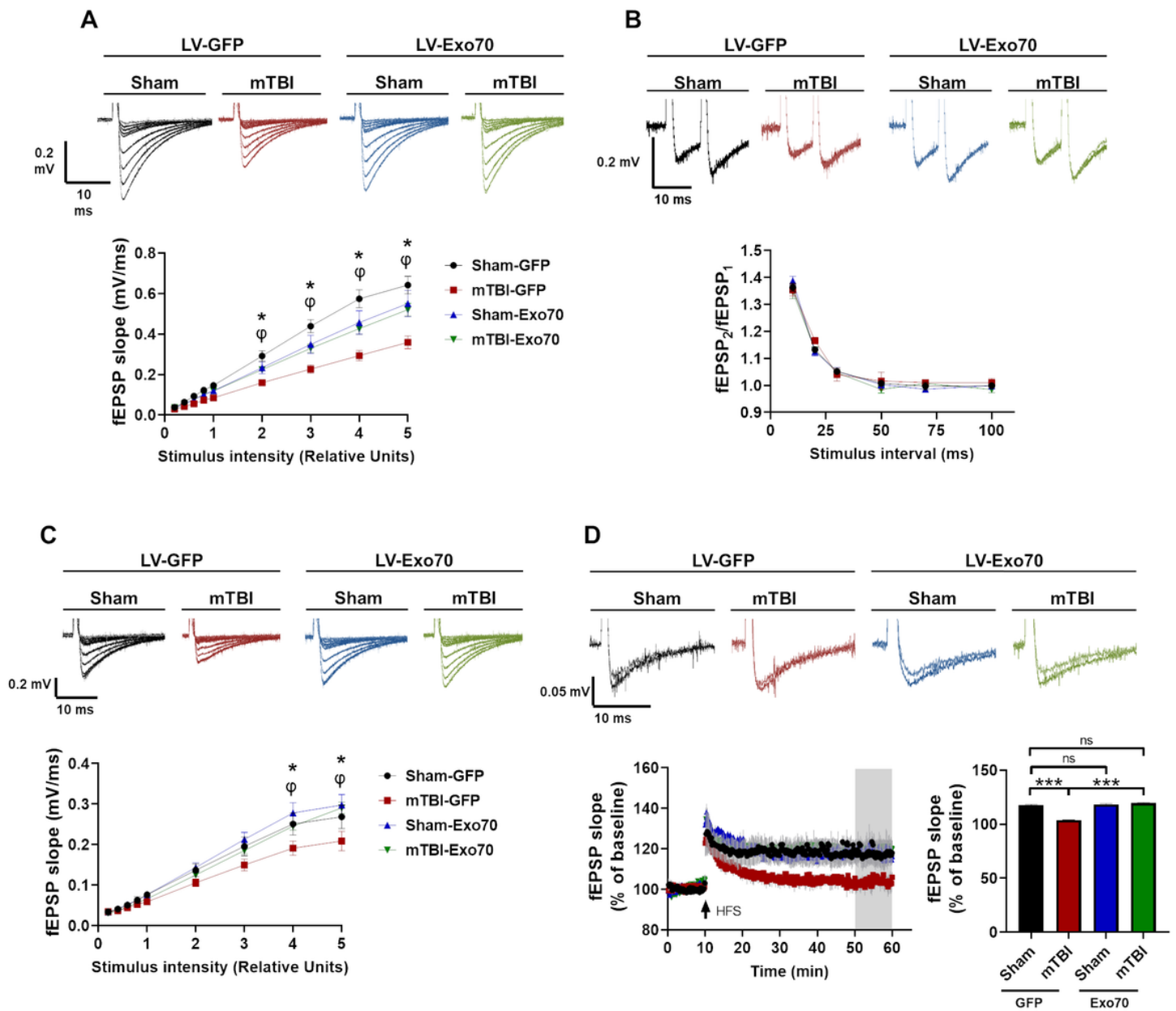


Figure 4

Synaptic transmission damage is protected by Exo70 overexpression. (A) Basal synaptic transmission in hippocampus from mTBI mice expressing GFP or Exo70. fEPSP slope induced by the input-output protocol to record total responses of CA3-CA1 synapses. Crescent stimuli recorded responses. (B) Paired pulse facilitation (PPF) of fEPSP shows no alterations in presynaptic activity in CA3-CA1 synapses. (C) NMDAR-related synaptic transmission in hippocampus from mTBI mice expressing GFP or Exo70. Recordings were made by incubating slices with 20 μ M NBQX. fEPSP slope induced by the input-output protocol to record NMDAR responses of CA3-CA1 synapses. Crescent stimuli recorded responses. (D) LTP was generated by high-frequency stimulation (HFS) in the hippocampal CA1 area, and the recording was carried out for 50 min. Quantification of fEPSP slope in the last 10 minutes of the recording. All graph values represent means \pm SEM, n = 6 slices per experimental group. Statistical differences were calculated by repeated measures ANOVA, followed by post hoc Bonferroni's test. Sham-GFP/TBI-GFP comparison:

* $p < 0.05$. TBI-GFP/TBI-Exo70 comparison: $\varphi p < 0.05$. The bar graph was analyzed using one-way ANOVA with Bonferroni's correction. *** $p < 0.001$.

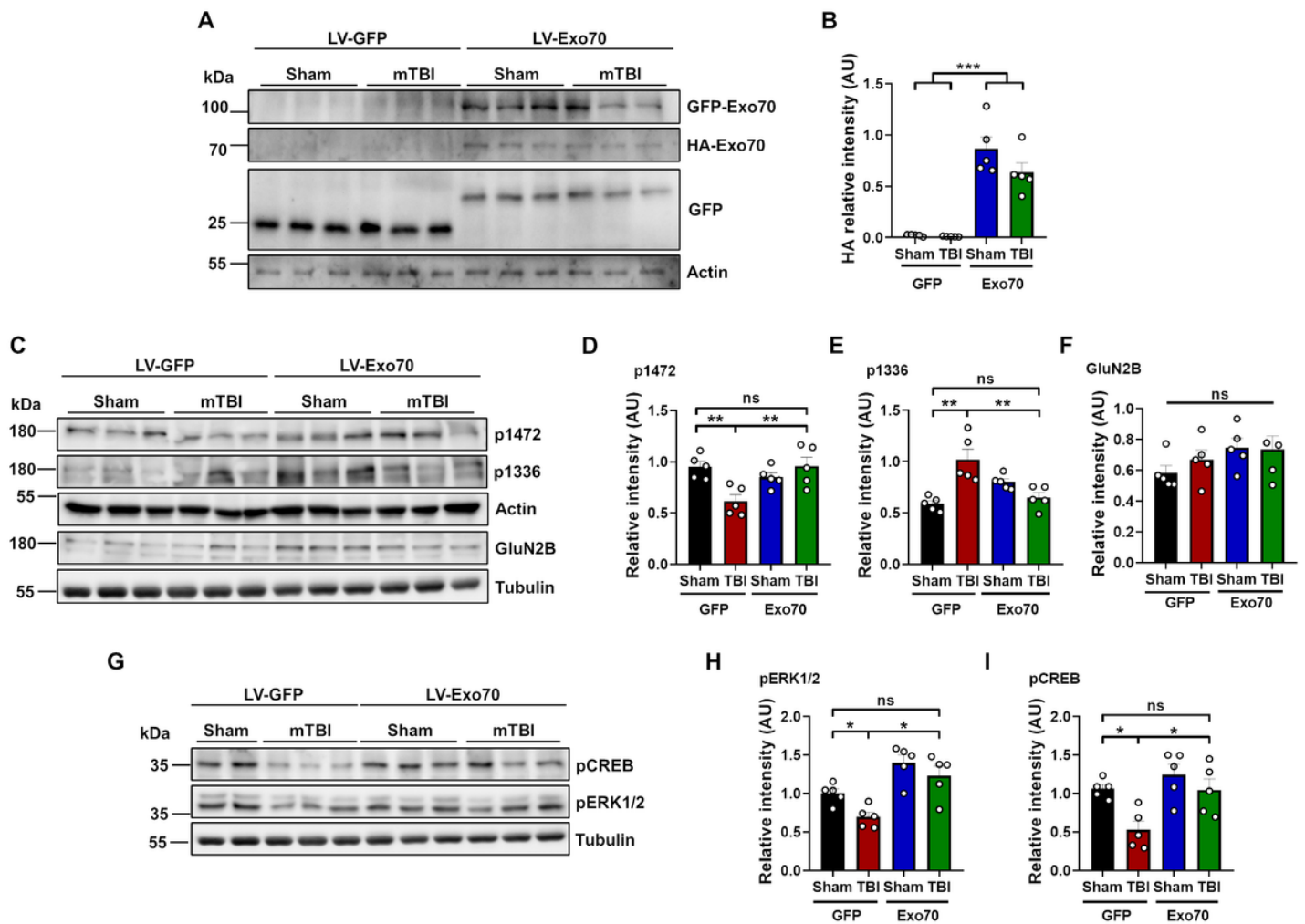


Figure 5

Exo70 overexpression reinforces NMDAR synaptic availability upon mTBI induction. Samples from the dorsal hippocampus were analyzed by western blot. 30 μg of protein samples were resolved in a 10% SDS-PAGE and transferred to PVDF membranes. Tubulin and Actin were used as a loading control. **(A)** Characterization of the lentiviral expression in all experimental groups using GFP y HA antibodies. **(B)** Densitometric analysis of HA-Exo70. **(C)** NMDAR synaptic localization after mTBI in injected mice. Samples were analyzed using GluN2B p1472, GluN2B p1336, and total GluN2B antibodies. **(D-F)** Densitometric analysis normalized with loading controls prior to normalization with Sham-GFP control samples. **(G)** NMDAR synaptic signaling after mTBI induction in Exo70-overexpressing samples. Samples were analyzed using pCREB and pERK1/2 antibodies. **(H and I)** The graphs show the densitometric analysis normalized with loading controls before normalization with Sham-GFP control samples. Values represent means \pm SEM, $n = 5$ mice per experimental group. Statistical differences were calculated by multiple comparison ANOVA, followed by post hoc Bonferroni's test. * $p < 0.05$, ** $p < 0.01$.

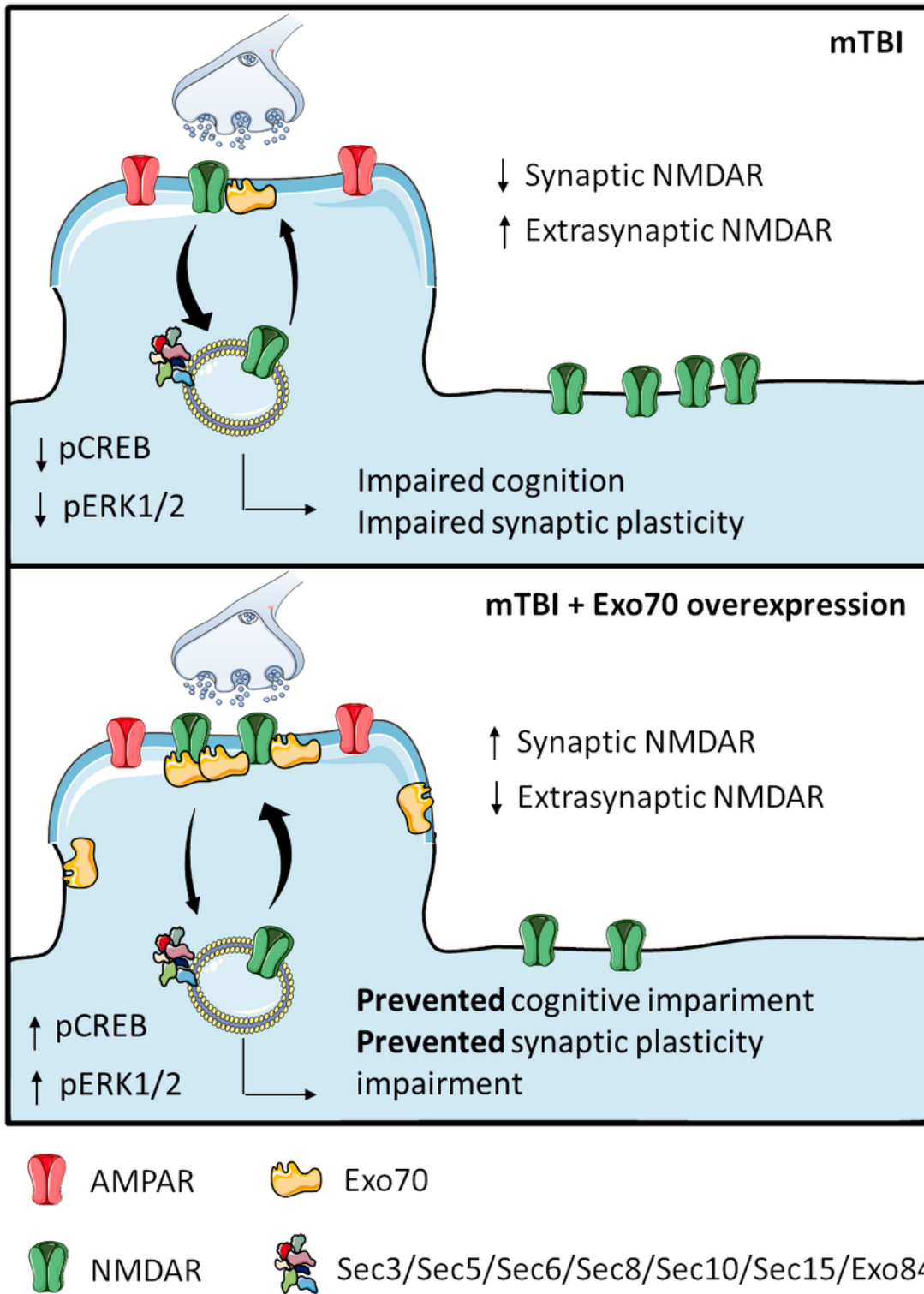


Figure 6

Schematic summary of Exo70 overexpression effects in our mTBI model.